Fourier transform emission spectroscopy of some new bands of ReN

R.S. Ram [a,*], P.F. Bernath [a,b,c], W.J. Balfour [d]

[a] Department of Chemistry, University of Arizona, Tucson, AZ 85721, USA
[b] Department of Chemistry, University of York, Heslington, York YO10 5DD, UK
[c] Department of Chemistry, University of Waterloo, Waterloo, Ont., Canada N2L 3G1
[d] Department of Chemistry, University of Victoria, Victoria, BC, Canada V8W 3V6

Abstract

The emission spectrum of ReN has been reinvestigated in the visible region using a Fourier transform spectrometer. Two new bands have been identified with band origins near 22 110 and 22 224 cm^{-1}. These bands have a common lower state and have been assigned as the 0^+–$A1$ and 0^-–$A1$ transitions. After rotational analysis it was noted that the new 0^+–$A1$ transition also has its upper state in common with the upper state of the $[24.7]0^+$–$X0^+$ transition reported previously [W.J. Balfour, J. Cao, C.X.W. Qian, S.J. Rixon, J. Mol. Spectrosc. 183 (1997) 113–118.]. This observation provides $T_{00} = 2616.26$ cm^{-1} for the $A1$ state. It is likely that the $A1$ and $X0^+$ states are two spin components of the $^3\Sigma^-$ ground state.
© 2007 Elsevier Inc. All rights reserved.

Keywords: Fourier transform spectroscopy; High resolution electronic spectroscopy; Diatomic transition metal nitrides

1. Introduction

In recent years there has been interest in the study of transition metal nitrides because of their importance in catalysis, surface science, ab initio calculations and organometallic chemistry [1–5]. The diatomic transition metal nitrides serve as simple models for the study of metal–nitrogen bonding in inorganic chemistry. The experimental data on these molecules are being used to test the quality of ab initio calculations aimed at predicting the spectroscopic properties of small molecules accurately. In the last few years, considerable progress has been made in the study of ReN. The first observation of ReN was made in 1994 [6] when a $\Delta\Omega = 1$ transition assigned as $[23.8]1$–$X0^+$, was observed near 23 746 cm^{-1} using Fourier transform emission spectroscopy as well as pulsed dye laser excitation spectroscopy. It was concluded that the $X0^+$ state was the ground state of ReN since this transition was also observed in the laser excitation experiments. In subsequent studies at

the University of Victoria, additional transitions were observed using laser excitation of molecules produced in a laser-ablation source [7,8]. A number of bands observed in the 375–542 nm region were rotationally analyzed and classified into five electronic transitions [7]. The lifetimes were also measured for the excited states. It was noted that a band observed at 540 nm, labeled as $[18.5]1$–$X0^+$, showed an unusual profile due to extra branches and had an irregular energy pattern because of strong perturbations in the excited state [8]. A deperturbation analysis of this band was performed and dispersed fluorescence spectra were recorded for all previously observed excited states [8], which revealed the presence of a number of low-lying states below 12 000 cm^{-1}. The Ω values for these states were established and are consistent with the electronic structure of ReN proposed in earlier studies. The approximate location of the expected low-lying states, $X^3\Sigma_1^-$, $^3\Delta_3$, $^3\Delta_2$, $^3\Delta_1$, and $^1\Sigma_0^+$ were determined from the dispersed fluorescence study. This work provided the location of an $\Omega = 1$ state at 2630 ± 100 cm^{-1} above the ground state, which is probably the lower state of the two transitions observed in the present study.

More recently ReN molecules were produced by Zhou and Andrews [9] by the reaction of laser ablated rhenium atoms with nitrogen and the fundamental band of ReN was measured in an N_2 matrix at 10 and 20 K providing a ground state vibrational interval close to the gas phase value [6]. In another study the high-resolution laser induced fluorescence spectra of ReN were recorded with a laser ablation/molecular beam spectrometer by Steimle and Virgo [10] and the (0,0) band of the $[26.0]0^+–X0^+$ system of ReN was investigated in the presence of an electric field. Ground and excited state electric dipole moments of 1.96(8) and 3.53(4) D, respectively, were determined for ^{187}ReN [10].

In the present work we report the observation of two new 0–0 bands near 22 110 and 22 224 cm^{-1} having their lower state in common. The 22 110 cm^{-1} band also has its upper state in common with the $[24.7]0^+–X0^+$ transition. This observation locates the lower $\Omega = 1$ state at 2616.26 cm^{-1} above the ground state.

2. Experimental

The experimental method and conditions for the observation of ReN bands have been provided in our previous paper [6]. Briefly, the molecules were produced in a rhenium hollow cathode lamp operated at 300 V and 457 mA current. A slow and continuous flow of a mixture of about 3 Torr of Ne and 5 mTorr of N_2 was maintained through the lamp in order to observe the ReN bands. The spectra were recorded using the 1-m Fourier transform spectrometer of the National Solar Observatory at Kitt Peak. The spectra in the 10 000–29 000 cm^{-1} region were recorded in two parts. The 10 000–19 500 cm^{-1} region was recorded using a UV beam splitter, Si-diode detectors and RG495 red pass filters while the 17 000–29 000 cm^{-1} region was recorded using the same beam splitter, Si-diode detectors and $CuSO_4$ filters. In both the experiments the spectra were recorded at a resolution of 0.02 cm^{-1}.

The spectra were measured using a data reduction program called PC-DECOMP developed by J. Brault at the National Solar Observatory and calibrated using the measurements of the Ne atomic lines made by Palmer and Engleman [11]. The new bands appear with very weak intensity (S/N ratio of ~4) and are partly overlapped by the spectra of much stronger N_2^+ lines. The precision of measurements of strong and unblended lines of ReN is expected to be of the order of ±0.005 cm^{-1}.

3. Results and discussion

Our FTS spectrum consists of two new and very weak bands of ReN in the 22 000–22 250 cm^{-1} region, in addition to the bands reported previously [6]. A part of the spectrum with the R heads of the two 0–0 bands marked is presented in Fig. 1. Although the band heads are weak, the branches were identified easily using a Loomis–Wood program. The structure of both these bands consists of P, Q and R branches with the Q branch being the most intense. The rotational assignment in the two bands was made by comparing the combination differences. This analysis indicates that the two bands have a common lower state, which has been identified as an $\Omega = 1$ state with small Ω-doubling constants. From this analysis we also conclude that the upper states of the two bands do not have any combination defects, consistent with an $\Omega = 0$ assignment. Based on rotational analysis, the new bands at 22 110 and 22 224 cm^{-1} have been labeled as $0^+–A1$ and $0^-–A1$ transitions. A comparison of the rotational constants of the new states to the values for other states reported previously by Balfour and coworkers [7,8], suggests that 22 110 and 24 706 cm^{-1} bands probably also have a common upper state. It was noted that the $0^+–A1$ transition was also observed by Cao et al. [8] in their dispersed fluorescence study. The $0^-–A1$ transition at 22 224 cm^{-1} has been observed for the first time. The Re atom has two naturally occurring isotopes ^{185}Re (37.07%) and ^{187}Re (62.93%). The absence of any isotope splitting in the two bands indicates that both bands are 0–0 bands. A part of the spectrum of the 22 110 cm^{-1} band is shown in Fig. 2 where some lines
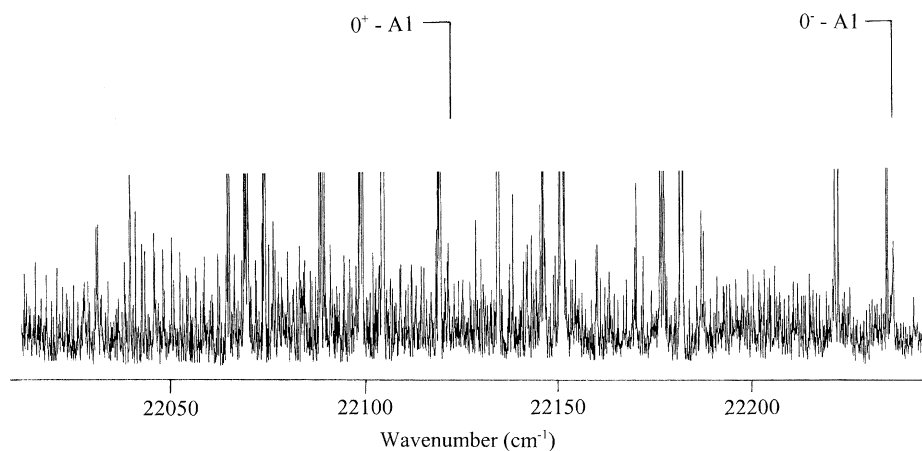

Fig. 1. A compressed portion of the emission spectrum of ReN marking the R heads of the $0^+–A1$, 0–0 and $0^-–A1$, 0–0 bands of ReN. Many of the strongest features are Re atomic lines.
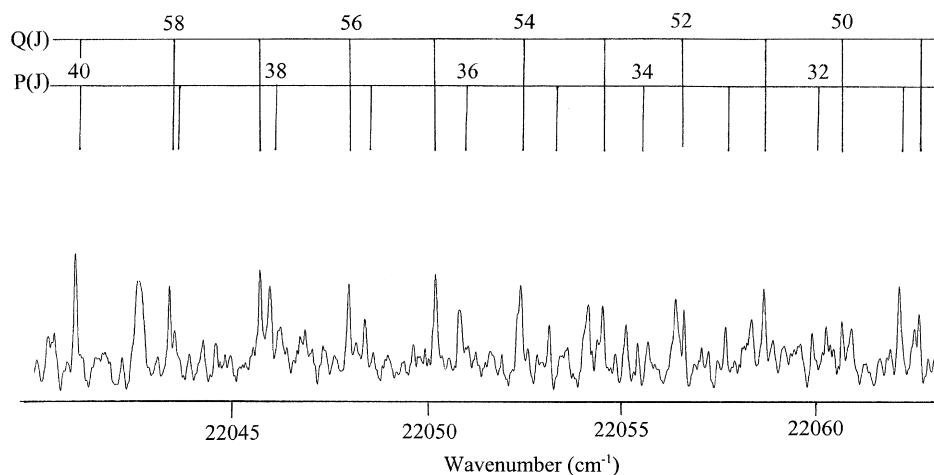
Fig. 2. An expanded portion of the 0^+–$A1$, 0–0 band of ReN, marking some rotational lines in the Q and P branches.

of the Q and P branches have been marked. The rotational lines were sorted out into branches using a color Loomis–Wood program running on a PC computer. The spectroscopic constants were determined by fitting the observed line positions to the following customary energy level expression:(for the $\Omega = 0^+$ and 0^- states)

$$F_v(J) = T_v + B_v J(J+1) - D_v[J(J+1)]^2 \qquad (1)$$

(for the $\Omega = 1$ state)

$$F_v(J) = T_v + B_v J(J+1) - D_v[J(J+1)]^2 + H_v[J(J+1)]^3 \pm 1/2\{q_v J(J+1) + q_{Dv}[J(J+1)]^2\} \qquad (2)$$

In the final fit the rotational lines of the [23.8]1–$X0^+$, 0–0 band [6] and [24.7]0^+–$X0^+$, 0–0 band [7] were also included with our data. The rotational lines of the [24.7]0^+–$X0^+$ transition were given slightly reduced weights due to a larger uncertainty in measurements, compared to the FTS spectra. The current FTS measurements were given weights based on their signal-to-noise ratio and extent of blending. Lines affected by perturbations were given lower weights or were deweighted. Two sets of spectroscopic constants were obtained by fitting the combined data. In the first fit all the states were treated as case (c) states. The observed lines positions in the new bands are reported in Table 1, where O–C refers to the observed minus calculated differences based on constants obtained from the case (c) fit. In the second fit the $X0^+$ and $A1$ states were treated as the components of the case (a), $X^3\Sigma^-$ state. An explicit listing of the matrix elements for the $^3\Sigma^-$ Hamiltonian can be found in our previous paper on NH [12]. The case (c) and case (a) constants obtained from our fits are provided in Tables 2 and 3, respectively, where the spectroscopic constants for the [23.8]1 state are also provided. The constants of the $X0^+$ and [23.8]1 states have changed slightly compared to those in reference 6, after combining with the data of other transitions.

The electronic spectra of ReN have been studied in great detail by Balfour and coworkers [7,8] and an overview of the electronic structure of the low-lying states is already available. From these studies it was concluded that the ground state of ReN is an $\Omega = 0^+$ state, a spin component of the $X^3\Sigma^-$ state arising from the $\delta^2\sigma^2$ configuration. Here the δ and σ orbitals are essentially non-bonding correlating with $5d$ and $6s$ atomic orbitals, respectively, of the Re atom [7]. From the dispersed fluorescence study, it was suggested that the $\Omega = 1$ component of the $X^3\Sigma^-$ state is located at about 2600 ± 100 cm^{-1} above the ground state. In addition, the approximate location of the three components of the low-lying $^3\Delta$ state arising from the $\delta^3\sigma^1$ configuration and the $^1\Sigma^+$ state, most probably arising from the $\delta^2\sigma^2$ configuration, were also provided (Table 2 of Ref. [8]). The current term value of 2616.26 cm^{-1} determined for the $\Omega = 1$ state agrees well with the value determined in the dispersed fluorescence study [8]. The large splitting between the $\Omega = 0^+$ and $\Omega = 1$ components is supported by large spin-orbit interaction of $\sim$2545 cm^{-1} for the rhenium atom [13]. The large spin orbit splitting also suggests that the different Ω states of ReN probably have a tendency towards Hund's case (c) coupling.

The rotational constants of 0.481100 and 0.480888 cm^{-1} for the $X0^+$ and $A1$ states are very similar in magnitude, consistent with their assignment as $X^3\Sigma_{0+}$ and $X^3\Sigma_1$ components of the $X^3\Sigma^-$ ground state. The two excited $\Omega = 0^+$ and $\Omega = 0^-$ states also have similar rotational constants of 0.461679 and 0.460407 cm^{-1}, respectively, and are separated by only $\sim$114 cm^{-1}. It is possible that the two states are also related. For example, an assignment as $^3\Pi_{0+}$ and $^3\Pi_{0-}$ is a possibility for the two new states although it is difficult to draw any definite conclusion based only on the present observations. As pointed out above, the electronic states of ReN have a tendency towards Hund's case (c) coupling, and the two states may very well be spin components of different states. There are no theoretical

Table 1
Observed line positions (in cm^{-1}) in the 0^+–$A1$, 0–0 and 0^-–$A1$, 0–0 bands of ReN

J	0^+–$A1$						0^-–$A1$					
	R(J)	O − C	Q(J)	O − C	P(J)	O − C	R(J)	O − C	Q(J)	O − C	P(J)	O − C
4			22109.453	−1					22223.939	−9		
5			22109.260	−3								
6			22109.006	−28					22223.477	−18		
7			22108.757	−9					22223.196	−10		
8			22108.458	−3					22222.855	−21		
9			22108.116	−1					22222.500	−5		
10			22107.737	2					22222.071	−22		
11			22107.311	−4					22221.610	−29		
12			22106.848	−8					22221.114	−31		
13			22106.355	−4	22094.293	−21			22220.562	−47		
14			22105.817	−7	22092.847	−2			22219.954	−78		
15			22105.245	−5	22091.335	−11			22219.291	−122		
16					22089.813	9			22218.421	−332		
17									22218.255	203		
18			22103.293	−5	22086.592	−11			22217.407	98		
19			22102.570	0	22084.934	−11			22216.593	68		
20			22101.817	13	22083.243	−5			22215.746	47		
21			22109.000	0	22081.511	0			22214.866	34		
22			22100.162	6	22079.735	1			22213.952	28		
23			22099.287	13	22077.918	−4			22213.000	25		
24					22076.071	3			22212.007	24	22190.063	11
25			22097.397	4					22210.969	19	22188.109	−5
26	22121.091	−28	22096.399	5	22072.244	−1			22209.893	16	22186.150	16
27	22120.974	−14	22095.357	0	22070.284	9			22208.764	4	22184.118	4
28	22120.828	11	22094.293	12	22068.268	3			22207.608	5	22182.078	25
29	22120.613	7	22093.173	8	22066.212	−3	22234.205	3	22206.407	3	22179.958	6
30	22120.375	19	22092.014	3	22064.145	17			22205.165	1	22177.812	3
31	22120.061	−5	22090.811	−7					22203.858	−24		
32	22119.735	0	22089.592	7	22059.848	14	22233.160	10	22202.561	3	22173.423	22
33					22057.640	13	22232.709	−8	22201.186	−6	22171.124	−11
34			22087.005	4	22055.380	−2	22232.240	−1	22199.784	−1	22168.840	11
35	22118.514	11	22085.650	−1	22053.109	13	22231.727	3	22198.333	−3	22166.496	14
36	22117.991	−20	22084.270	9	22050.792	21	22231.170	4	22196.832	−13	22164.102	8
37	22117.475	−4	22082.831	0	22048.416	10	22230.574	8	22195.307	−5	22161.672	6
38	22116.912	5	22081.369	8	22045.999	−3	22229.927	4	22193.727	−10	22159.213	19
39	22116.293	−1	22079.854	2	22043.571	13	22229.246	6	22192.110	−11	22156.692	5
40	22115.643	3	22078.308	5	22041.067	−7	22228.524	9	22190.456	−6	22154.157	27
41	22114.950	3	22076.735	21	22038.556	6	22227.752	4	22188.749	−13	22151.515	−11
42	22114.203	−7	22075.108	23	22035.988	2	22226.927	−11	22187.027	7	22148.896	−5
43	22113.421	−13	22073.427	10	22033.378	−4	22226.078	−9	22185.229	−6	22146.239	14
44	22112.612	−5	22071.720	12	22030.735	−3	22225.182	−12	22183.406	−2	22143.506	−2
45	22111.753	−6	22069.964	5	22028.041	−12	22224.255	−3			22140.743	−6
46	22110.875	16	22068.169	0	22025.306	−23	22223.276	−5	22179.628	0	22137.956	6
47	22109.907	−11	22066.345	5	22022.561	−2	22222.257	−4	22177.665	−10	22135.097	−11
48	22108.916	−19			22019.752	−6	22221.198	−2	22175.673	−6	22132.229	3
49	22107.893	−19	22062.554	−4	22016.894	−17	22220.071	−24	22173.645	4	22129.304	3
50	22106.848	3	22060.598	−8	22014.007	−17	22218.950	2	22171.561	0	22126.329	−7
51	22105.714	−24	22058.616	2	22011.096	0	22217.757	−2	22169.440	2	22123.336	6
52			22056.572	−9	22008.109	−19	22216.521	−7	22167.283	10	22120.270	−11
53	22103.379	−17	22054.494	−12	22005.109	−8	22215.254	−1	22165.072	7	22117.191	0
54	22102.122	−40	22052.382	−9	22002.037	−29	22213.952	14	22162.820	5	22114.051	−8
55	22100.847	−39	22050.211	−23	21998.940	−35	22212.583	4	22160.520	−2	22110.875	−11
56	22099.525	−43	22048.000	−36	21995.786	−55	22211.179	2	22158.193	7	22107.679	8
57			22045.745	−51	21992.613	−53	22209.735	2	22155.808	0		
58			22043.439	−76	21989.380	−70	22208.246	1	22153.395	8	22101.101	−15
59			22041.067	−125	21986.111	−81	22206.724	9			22097.768	−8
60							22205.165	23	22148.425	9	22094.388	−5
61							22203.513	−13	22145.862	−4	22090.973	3
62			22034.071	99			22201.870	3	22143.282	9	22087.497	−6
63			22031.542	61			22200.165	1	22140.641	4	22083.993	−3
64			22028.993	45			22198.405	−13	22137.956	−2	22080.450	5
65			22026.405	33			22196.633	3	22135.240	4	22076.842	−11

Table 1 (*continued*)

J	0^+–A1						0^-–A1					
	R(J)	O − C	Q(J)	O − C	P(J)	O − C	R(J)	O − C	Q(J)	O − C	P(J)	O − C
66			22023.789	36			22194.769	−27	22132.473	3	22073.226	7
67			22021.111	19			22192.941	20	22129.664	3		
68			22018.409	20			22190.968	−34	22126.807	−2		
69			22015.652	11			22189.014	−25	22123.915	2	22062.047	−15
70			22012.869	17			22187.027	−6	22120.974	0	22058.255	−3
71			22010.033	15			22184.979	−3	22117.991	0		
72			22007.147	6			22182.886	−2	22114.950	−15	22050.537	13
73			22004.223	3			22180.756	6	22111.871	−24	22046.591	−1
74			22001.258	2							22042.624	6
75			21998.251	4							22038.624	22
76											22034.543	1
77			21992.100	0							22030.448	8
78			21988.966	8							22026.284	−10
79			21985.767	−5							22022.091	−15
80			21982.532	−10							22017.881	5
81			21979.274	7								
82			21975.951	4								
83			21972.568	−15								
84			21969.174	2								
85			21965.714	−1								
86			21962.216	2								

Note. O − C are observed minus calculated values in the units of 10^{-3} cm^{-1}.

Table 2
Case (c) spectroscopic constants (in cm^{-1}) for the $X0^+$, A1, [23.8]1, 0^+ and 0^- states of ReN

Constants[a]	$X0^+$	A1	[23.8]1	0^+	0^-
T_{00}	0.0	2616.263(11)	23746.4178(12)	24726.098(11)	24840.623(11)
B_0	0.481100(25)	0.480888(14)	0.439780(25)	0.461679(14)	0.460407(14)
$10^7 \times D_0$	3.922(82)	3.384(20)	4.704(80)	4.245(19)	3.783(20)
$10^{12} \times H_0$	3.76(83)	—	3.11(80)	—	—
$10^4 \times q_0$	—	2.4589(38)	−4.738(12)	—	—
$10^9 \times q_{D0}$	—	—	5.194(26)	—	—

[a] Values in parentheses are one standard deviation in the last digits quoted.

Table 3
Case (a) spectroscopic constants (in cm^{-1}) for the $X^3\Sigma^-$, [23.8]1, 0^+ and 0^- states of ReN

Constants[a]	$X^3\Sigma^-$	[23.8]1	0^+	0^-
T_{00}	0.0	22002.3830(74)[b]	22982.0294(39)[b]	23096.5547(44)[b]
B_0	0.4809566(75)	0.439641(11)	0.4617418(71)	0.4604696(71)
$10^7 \times D_0$	3.499(13)	4.313(12)	4.340(12)	3.880(13)
$10^{13} \times H_0$	2.20(63)	—	—	—
$10^4 \times q_0$	—	−4.742(12)	—	—
$10^9 \times q_{D0}$	—	5.33(25)	—	—
$10^1 \times \gamma_0$	1.5314(71)	—	—	—
λ_0	1308.5154(54)	—	—	—
$10^4 \times \lambda_{D0}$	−1.862(44)	—	—	—

[a] Values in parentheses are one standard deviation in the last digits quoted.
[b] The T_{00} values are different from those in Table 2 since the zero energy is different for the case (a) fit.

predictions available for ReN to help in the electronic assignment of the observed Ω states.

Our analysis indicates that excited states of both transitions are affected by local perturbations. The 0^+–A1, 0–0 band at 22110 cm^{-1} is perturbed near J = 60 while the 0^-–A1, 0–0 band at 22224 cm^{-1} is affected by perturbations near J = 16. Several Ω = 0 and 1 states which have

been observed [7,8] in the vicinity of the two states may be responsible for these perturbations.

4. Conclusion

Two new emission bands of ReN, having a common Ω = 1 lower state, have been observed in the 21000–

22 500 cm^{-1} region using a Fourier transform spectrometer. These bands have been assigned as the 0–0 bands of the 0^+–$A1$ and 0^-–$A1$ transitions of ReN. The 22 110 cm^{-1} band also has its upper state in common with the $[24.7]0^+$–$X0^+$ transition observed previously by Balfour et al. [7,8]. This observation places the $A1$ state at 2616.26 cm^{-1} above the ground $X0^+$ state. The common lower state, $A1$, is most probably the $\Omega = 1$ spin component of the $X^3\Sigma^-$ ground state of ReN. This work provides improved spectroscopic constants for the first excited state, $A1$, of ReN.

Acknowledgment

References

[1] F.A. Cotton, G. Wilkinson, C.A. Murillo, M. Bochmann, Advanced Inorganic Chemistry, A Comprehensive Text, Wiley, New York, 1999.

[2] N.N. Greenwood, A. Earnshaw, The Chemistry of the Elements, Pergamon Press, Oxford, 1990.

[3] D.R. Lide, CRC Handbook of Chemistry and Physics, 73rd ed., CRC Press, Boca Raton, 1992.

[4] F. Gassner, E. Dinjus, H. Gorls, W. Leitner, Organometallics 15 (1996) 2078–2082.

[5] M.A. Casado, J.J. Perez-Torrente, M.A. Ciriano, L.A. Oro, A. Orejon, C. Claver, Organometallics 18 (1999) 3035–3044.

[6] R.S. Ram, P.F. Bernath, W.J. Balfour, J. Cao, C.X.W. Qian, S.J. Rixon, J. Mol. Spectrosc. 168 (1994) 350–362.

[7] W.J. Balfour, J. Cao, C.X.W. Qian, S.J. Rixon, J. Mol. Spectrosc. 183 (1997) 113–118.

[8] J. Cao, W.J. Balfour, C.X.W. Qian, J. Phys. Chem. A 101 (1997) 6741–6745.

[9] M. Zhou, L. Andrews, J. Phys. Chem. A 102 (1998) 9061–9071.

[10] T.C. Steimle, W.L. Virgo, J. Chem. Phys. 121 (2004) 12411–12420.

[11] B.A. Palmer, R. Engleman, Atlas of the Thorium Spectrum, Los Alamos National Laboratory, Los Alamos, 1983.

[12] C.R. Brazier, R.S. Ram, P.F. Bernath, J. Mol. Spectrosc. 120 (1986) 381–402.

[13] H. Lefebvre-Brion, R.W. Field, Perturbations in the Spectra of Diatomic Molecules, Academic Press, Inc., Orlando, 1986.